UCRL-JRNL-203527

LAWRENCE
LIVERMORE
NATIONAL
LABORATORY

Ab Initio Study of Al(III) Adsorption on Stepped {100} Surfaces of KDP Crystals

E. A. Salter, A. Wierzbicki, and T. Land

April 15, 2004

Submitted to: The Journal of Structural Chemistry

Disclaimer

Ab initio Study of Al(III) Adsorption on Stepped {100} Surfaces of KDP Crystals

E. A. Salter[a], A. Wierzbicki[a,*], and T. Land[b]

[a]*Department of Chemistry, University of South Alabama, Mobile, AL 36688, USA*
[b]*Lawrence Livermore National Laboratory, Livermore , CA 94550, USA*

Abstract

Crystals of potassium dihydrogen phosphate (KH_2PO_4, KDP) are grown in large scale for use as nonlinear material in laser components. Traces of trivalent metal impurities are often added to the supernatant to achieve habit control during crystal growth, selectively inhibiting the growth of the {100} face. Model systems representing $AlPO_4$-doped KDP {100} stepped surfaces are prepared and studied using ab initio quantum methods. Results of Hartree-Fock partial optimizations are presented, including estimated energies of ion pair binding to the steps. We find that the PO_4^{3-} ion takes a position not unlike that of a standard phosphate in the crystal lattice, while the aluminum atom is displaced far from a K^+ ion position to establish coordinations with the PO_4^{3-} ion and to bind with another lattice-bound phosphate. Our optimized structures suggest that it is the formation of a fourth coordination of Al(III) to a third phosphate ion from solution, or perhaps from a nearby position in the lattice, that disrupts further deposition, pinning the steps.

Background

Potassium dihydrogen phosphate (KH_2PO_4, KDP) crystals have important uses as nonlinear material in laser components. The National Ignition Facility at Lawrence Livermore National Laboratory requires large single-crystal plates for Q-switches and second harmonic generation (SHG), and KDP crystals are currently being grown in large-scale for these purposes.[1] The need for habit control during crystal growth has led to interest in the step-pinning mechanisms instigated by trivalent metal impurities which cause growth inhibition of the prismatic {100} face.[2]

Figure 1 illustrates the morphology of the KDP crystal: a tetragonal prism made of four prismatic {100} faces, capped by opposing tetragonal pyramids composed of {101} faces. The high-temperature (paraelectric phase) crystal structure of KDP belongs to the tetragonal space group $I\bar{4}2d$ and the $\bar{4}2m$ point group.[3] Since hydrogen bonds link each oxygen of every phosphate ion with an oxygen of a neighboring phosphate, KDP is characterized by a three-dimensional continuous network of hydrogen-bonded phosphate ions. The crystal lattice can be viewed as a stacked array of columns, which we refer to here as "H columns", all parallel to the <001> vector. Each "H column" is an alternating cation-anion in-line sequence in which each K^+ ion is doubly coordinated to the phosphate on either side of it with a distance of $d(K^+\text{-}O) = 2.90$ Å. Each K^+ ion in the body of the lattice has four additional "nearest neighbor" oxygen interactions. The "H columns" are interlinked by these K^+-O interactions with $d(K^+\text{-}O) = 2.83$ Å. The X-ray diffraction unit cell parameters[3] are a=b=7.4521(4) Å, c=6.974(2) Å and $\alpha=\beta=\gamma=90°$, with four formula units per cell. P and K atoms occupy the special positions (0,0,0) and (0,0,1/2), respectively, and the H and O atoms are in general positions (x,y,z). Protons of each hydrogen bond are distributed equally over two equilibrium positions with 50% occupations each. Their positions are related by a two-fold rotation axis, and since they are crystallographically equivalent, they are indistinguishable in diffraction experiments.

It is well known that traces of trivalent metal impurities such as Fe^{3+}, Cr^{3+}, and Al^{3+} in solution inhibit growth of the prismatic {100} faces of KDP but have little effect on the growth of the pyramidal {101} faces.[2] Indeed, the growth of prismatic faces is almost completely suppressed under conditions of low supersaturation in the presence of these ions.[4,5] Moreover, the concentration of these impurities is found to be one to two orders of magnitude higher in the prismatic versus the pyramidal sectors.[5,6] This selectivity has been attributed to the fact that the {101} surface layer is K^+-terminated, as shown by grazing incidence X-ray diffraction, and thus a large barrier should exist for adsorption of a multivalent cation.[7] In contrast, the {100} face has both K^+ and $H_2PO_4^-$ ions at the solution interface and would presumably incorporate a multivalent metal impurity more readily.[7] The predominant Al(III) species in the supernatant is expected to be the neutral $AlPO_4$,[8] however, and a full explanation of the adsorption selectivity may be more complex. Nevertheless, the impurity is understood to locally pin the moving steps on the {100} surface.

Introduction

The orientations of some possible steps on the KDP {100} face are shown in Fig. 1. Only one kind of horizontal step seems important: the H step, which runs parallel to the previously described “H columns” and has a “H column” at the step edge. From Fig. 1 it should be clear that the riser of the H step is another prismatic {100} face. Several vertical or diagonal steps are possible; the edges of these steps are either occupied by a column of K^+ ions or by a column of $H_2PO_4^-$ ions. Vertical steps are of interest because they correspond to the experimentally observed direction of motion of steps in an oriented crystal, as reported in AFM studies.[9] Diagonal steps may be important because the risers of the diagonal steps are {101} surfaces.

In a prior investigation,[10] we studied the H step, two vertical steps (V and V'), and two diagonal steps (D and D') that are possibly present on the growing KDP {100} surface using ab initio quantum methods. We found that the steps terminated by phosphate ions, V' and D', are less energetically favorable than their K^+-terminated counterparts, V and D, according to our estimated ion removal and column removal energies. In steps V and D, oxygen atoms of the embedded phosphates extend to the step edges, limiting the exposure of the edge potassium ions. The riser of the D step is the K^+-terminated pyramidal {101} surface.

In this work, we present the results of ab initio quantum calculations on model systems representing three important Al(III)-doped KDP {100} steps: the H, V, and D steps. We assume that the PO_4^{3-} counter ion is present and doubly coordinated to the aluminum ion; that is, we initially place the Al•PO_4 ion pair along an "H column", a natural choice to achieve a double coordination. Our goals are to examine the binding of the dopant and its impact on the local structure of the steps, and to thereby identify plausible step-pinning mechanisms on the KDP {100} surface.

Method

A large slab (5x5x2) with a {100} surface was generated from the KDP unit cell[3] using Cerius4.2[11] software. Because of the hydrogen bonding in the KDP crystal lattice, the phosphate ions of such a slab have apparent stoichiometry H_4PO_4, where each hydrogen atom location is 50% populated. It was necessary, therefore, to delete two hydrogen atoms from each phosphate group to produce a slab in which each phosphate group has exactly two covalently bonded hydrogen atoms and is engaged in exactly two hydrogen bonds (unless the phosphate lies on the slab surface). After these random deletions were made, neutral clusters $(KH_2PO_4)_n$ (n=12 to 14) were cut from the slab to produce small representations of stepped {100} surfaces. Adsorption of the metal impurity was mimicked by placing an Al^{3+} ion in a K^+ site on or near a step edge. A doubly coordinated

phosphate group was then selected and deprotonated to take role of the PO_4^{3-} ion; hydrogen atoms were shifted in the cluster so that all nearest neighbor oxygens to the Al^{3+} ion were left unprotonated. Our models of the doped H, V, and D steps are shown in Figs. 2-4. Ab initio Hartree-Fock[12] calculations were performed on a Cray SV1 supercomputer using the Jaguar[13] computational chemistry software. Partial optimizations were carried out to determine the equilibrium positions of the aluminum ion and the associated phosphate group(s). In the case of the H step, both phosphates coordinated to the Al^{3+} ion along the step edge were allowed to move. Binding energies were estimated from differences of single point energy calculations. All calculations employed the LACVD basis set, a double-zeta basis, which treats core electrons as effective core potentials.[14]

Results and Discussion

The Hartree-Fock optimized structures for the Al•PO_4-doped steps are shown in Figs. 2-4; estimated binding energies for the Al•PO_4 ion pair are shown in Table I. The optimized structure for the H step, Fig. 2, shows the aluminum atom to have four coordinations with oxygens of three different phosphate groups. Along the edge of the step, two oxygens of the PO_4^{3-} group doubly coordinate the aluminum atom with slightly assymmetric distances, d(Al-O) = 1.88 and 1.83 Å, to form what we identify as the ion pair. For comparison, a gas phase optimization for the isolated ion pair (C_{2v} symmetry) using the same basis set yields slightly shorter Al-O distances of 1.70 Å. The four-membered ring of the ion pair shown in Fig. 2 is slightly puckered; the O-P-O-Aldihedral is about 6°. A third coordination to Al(III) in Fig. 2 is made by a “nearest neighbor” oxygen of a phosphate in the adjacent “H column” on the upper terrace of the step. For this coordination, d(Al-O) = 1.81 Å. By comparison, these bonds are much shorter than the previously mentioned K^+-O distances of 2.90 and 2.83 Å, and so, the aluminum atom must move 1.4 Å from the initial K^+

location to achieve them. Also along the step edge, the $H_2PO_4^-$ ion to the right of the aluminum atom is pulled up from its normal lattice position to make a fourth coordination (d(Al-O) = 1.73 Å). The central P atom of the displaced phosphate is about 1.4 Å from its initial location, far out of alignment with a normal phosphate lattice position. Since the protonation state of the neighboring phosphate species may be expected to influence the aluminum atom's position and its coordinations and since the dislocation of this $H_2PO_4^-$ ion was so drastic, we carried out a test optimization in which two HPO_4^{2-} species sandwich the Al^{3+} ion. The final structure is essentially the same as that shown in Fig. 2. For this model arrangement, the HPO_4^{2-} on the right is uprooted in the same manner as the $H_2PO_4^-$ ion in Fig. 2 to make a single coordination with d(Al-O) = 1.68 Å. The double coordination distances with the HPO_4^{2-} on the left are somewhat more assymmetric, with d(Al-O) = 2.01 and 1.86 Å, while the distance of the remaining "nearest neighbor" bond to the lattice-bound phosphate is essentially the same as before. Adsorption of $AlPO_4$ into an H step, perhaps at a kink site, followed by the bonding of an additional phosphate ion to create the complex shown in Fig. 2, may be sufficient to stop further ion deposition and pin the moving step.

Two binding options for Al•PO_4 embedded in the V step are shown in Figs. 3a and b. In the first, Fig. 3a, the aluminum ion is placed initially at a K^+ ion position on the step edge. The final binding orientation is analogous to that of the H step, Fig. 2, without the phosphate ion to the right, of course. The three optimized Al-O bond distances for the V step in Fig. 3a are all about 1.82 Å. The aluminum ion has moved 1.3 Å from its initial position. The four-membered ring is puckered; the O-P-O-Al dihedral is about 13°. The fourth coordination position on Al(III) is clearly available for binding to another phosphate ion from solution; such a phosphate would extend out of the step edge and would be far out of alignment with its normal lattice position and serve as an impediment

to further growth of the terrace. In the second binding option, Fig. 3b, the PO_4^{3-} ion is placed at an outermost phosphate position (not quite on the step edge), and the Al^{3+} ion is placed at the nearest interior position. The optimized structure is essentially that of Fig. 3a, rotated by 180º. The single coordination distance is a slightly shorter with d(Al-O) = 1.79 Å versus 1.81 Å . In this case, if the fourth coordination position is taken by an additional adsorbed phosphate, deposition along the step would probably not be greatly affected since the optimized PO_4^{3-} ion position on the step edge is not significantly altered from the standard phosphate lattice position. The presence of the dopant (and perhaps an additional coordinated phosphate) might disrupt the growing layer above its position, but this also seems unlikely. In both V step options, only one Al-O bond needs to be broken to remove the ion pair, and our models estimate the Al•PO_4 binding energy to be about the same at roughly -270 kcal/mol (see Table I). By far, the strongest binding is found for the H step at -392 kcal/mol.

Figure 4 shows a putative binding orientation for Al•PO_4 embedded in the D step. The initial position of the Al^{3+} ion was along the step edge at a K^+ ion location. As in the doped V step, Al(III) establishes three bonds, with a fourth binding to an additional adsorbed phosphate still possible. Again, such a phosphate would be far out of the normal lattice position and would likely impede further deposition along the D step edge. The Al-O coordination distances to the PO_4^{3-} ion are 1.79 and 1.75 Å, and the Al-O bond distance involving the phosphate oxygen in the lower terrace is 1.76 Å. As in the bindings shown for the V step, only one Al-O bond needs to be broken to remove the Al•PO_4 ion pair. Table I shows that the binding energy is the weakest for this step.

Summary

We have carried out Hartree-Fock calculations on three stepped KDP {100} surfaces in order to gain an atomic-level understanding of step pinning caused by the presence of Al^{3+}. Under the assumption that $AlPO_4$ is the species that becomes embedded in the moving steps, we have

performed partial optimizations with Al^{3+} positioned at candidate doping sites in the steps. We find that when the PO_4^{3-} is positioned in the same "H column" in the lattice, a natural choice to achieve a double coordination with the Al^{3+} ion, the energy optimizations produce an identifiable Al•PO_4 ion pair. The bound Al•PO_4 ion pair generally resembles its free (gas phase) structure, with slightly longer double coordinations and somewhat nonplanar. We have estimated binding energies of the Al•PO_4 ion pair to these steps (Table I), and we find strong binding to the H step, relative to the binding for the V and D steps. We attribute this strong binding to the presence of two Al-O bonds to other phosphate oxygens of the lattice, Fig. 2, rather than just one, as in the doped V and D steps, Figs. 3 and 4. In all of our models, the PO_4^{3-} ion reaches an equilibrium position not unlike that of a standard position in the crystal lattice, while the aluminum atom is displaced far from a K^+ position (by about 1.3-1.4 Å) to make the two tight bonds with the PO_4^{3-} ion and to achieve a third coordination, anchoring to the oxygen of another lattice-bound phosphate. We propose that when the aluminum atom is located along a step edge as in Figs 2, 3a and 4, the formation of a fourth coordination with another phosphate from solution, or perhaps uprooted from the lattice (as explicitly shown in Fig. 2), is possible. This phosphate will be out of the lattice registry and will impede further deposition of ions along the step edge. In particular, we conclude that a complex like that shown in Fig. 3a for Al(III) bound to the V step (a step parallel to the <010> vector), may be the cause of the step-pinning observed by Sangwal and co-workers in AFM imaging of the KDP {100} surface.[9]

Acknowledgements

Work performed under the auspices of the U.S. Department of Energy by the University of California at Lawrence Livermore National Laboratory under contract No. W-7405-Eng-48. We thank the Alabama Supercomputing Authority for computational resources. Figures 2-4 were rendered using WebLab ViewerPro 3.5.

Table I. Estimated Al•PO_4 Binding Energies (kcal/mol) for Selected KDP {100} Steps[a]

STEP	Binding Energy
H	-392
V[b]	-269, -268
D	-186

[a]Orientations of the steps on the {100} face are indicated in Figure 1. Putative bindings of the Al•PO_4 ion pair to the steps are illustrated in Figs. 2-4. Binding energies were computed from single-point Hartree-Fock/LACVD energies after partial optimizations. The stoichiometry of the computational model clusters are given by $AlPO_4(KH_2PO_4)_n$ with n=12, 11, and 13 for steps H, V, and D, respectively.
[b]Two different positions of the ion pair in the V step were considered.

FIGURE CAPTIONS

Fig. 1. The KDP tetragonal prism: four prismatic {100} faces are capped by opposing tetragonal pyramids with {101} faces. The orientation of the horizontal (H), vertical (V) and diagonal (D) step edges on the {100} surface are indicated by dashed lines. The H step is parallel to the <001> vector; the V step is parallel to the <010> vector.

Fig. 2. Al•PO_4 embedded in the horizontal (H) step of KDP. The step edge is indicated by the dashed line. View is from above the {100} surface. Small balls and tube structures represent the respective K^+ and $H_2PO_4^-$ ions of the lower terrace; larger balls and ball-and-stick models represent the atoms of the upper terrace. Color scheme: Aluminum (gold), Potassium (blue), Phosphorous (orange), Oxygen (red), Hydrogen (gray). The "H columns", in-line sequences of alternating K^+ and $H_2PO_4^-$ ions, run from left to right. The Hartree-Fock optimized structure is shown. Three ions along the step edge were allowed to move during the minimization: the Al^{3+} ion, the PO_4^{3-} ion at left, and the $H_2PO_4^-$ ion at right. The initial location of the ions are indicated by wireframe structures; the Al^{3+} ion was initially placed in a K^+ ion lattice position on the step edge. In the final structure, the aluminum atom is shown to have four strong bonds. The aluminum atom has moved toward the PO_4^{3-} ion at left to establish a strong double coordination (forming the ion pair) and into the step face to bond with another phosphate belonging to the adjacent column of ions on the upper terrace. The PO_4^{3-} ion has turned to maintain the double coordination; its central P atom has moved only 0.3 Å from its initial lattice position. The $H_2PO_4^-$ ion at the right of the aluminum ion has been uprooted from its normal position along the step edge to establish a single strong coordination with the aluminum; its final position is almost directly above another phosphate of the lower terrace. The Al^{3+} ion and the central P atom of this $H_2PO_4^-$ ion are both about 1.4 Å from their respective initial positions. The final positions of all three optimized ions lie slightly above the upper terrace central plane. When two HPO_4^{2-} ions sandwich the Al^{3+} ion, the energy optimization yields essentially the same structure shown here.

Fig. 3a. Al•PO_4 embedded in the vertical (V) step of KDP. The step edge is indicated by the dashed line. View is from above the {100} surface. Color scheme and model representations are as in Fig. 2. The Hartree-Fock optimized structure is shown, in which two ions were allowed to move during the minimization: the Al^{3+} ion and the PO_4^{3-} ion at its left. The Al^{3+} ion was initially placed in a K^+ ion lattice position on the step edge. In the final structure, the aluminum atom is shown to have three strong coordinations. The aluminum has moved about 1.3 Å at an angle into the step face to establish a strong double coordination with the PO_4^{3-} ion and to bond with another phosphate ion near the step edge. The central P atom of the PO_4^{3-} ion has moved only 0.2 Å. The local geometry about the aluminum atom is analogous to that of Fig. 2, absent the one phosphate coordination at the right.

Fig. 3b. Alternative orientation of Al•PO_4 embedded in the vertical (V) step of KDP. View is from above the {100} surface. Color scheme and model representations are as in Fig. 2. The Hartree-Fock optimized structure is shown, in which two ions were allowed to move during the minimization: the Al^{3+} ion and the PO_4^{3-} ion at its right. The Al^{3+} ion was initially placed in a K^+ ion

lattice position on the upper terrace, but away from the step edge. In the final structure, the aluminum atom is shown to have three strong coordinations. The aluminum has moved a distance of 1.4 Å at an angle toward the step face to establish a strong double coordination with the PO_4^{3-} ion and to bond with another phosphate ion near the step edge; its final position is slightly above the upper terrace plane. The PO_4^{3-} ion has rotated slightly to maintain the double coordination; its central P atom has moved just 0.2 Å from its initial lattice position.

Fig. 4. Al•PO_4 embedded in the diagonal (D) step of KDP. The step edge is indicated by the dashed line. View is from above the {100} surface. Color scheme and model representations are as in Fig. 2. The Hartree-Fock optimized structure is shown, in which two ions were allowed to move during the minimization: the Al^{3+} ion and the PO_4^{3-} ion at its left. The Al^{3+} ion was initially placed in a K^+ ion lattice position on the step edge. In the final structure, the aluminum atom is shown to have three strong coordinations. The aluminum has moved toward the PO_4^{3-} ion to establish a strong, double coordination with it and has moved down to bond with another phosphate on the lower terrace. The PO_4^{3-} ion has moved to maintain the double coordination; its central P atom has moved 0.4 Å from its initial lattice position and lies slightly above the original plane.

REFERENCES

[1] J.D. Lindl, Phys. Plasmas 2 (1995) 3933.

[2] L.N. Rashkovich, KDP-family Single Crystals (Adam-Hilger, New York, 1991).

[3] R.J. Nelmes, Z. Tun, W.F. Kuhs, Ferroelectrics 71 (1987) 125.

[4] L.N. Rashkovich, N.V. Kronsky, J. Crystal Growth 182 (1997) 434.

[5] T. A. Land, J.J. De Yoreo, T.L. Martin, G.T. Palmore, Crystallography Reports 44 (1999) 655.

[6] N. Zaitseva, L. Carman, I. Smolsky, R. Torres, M. Yan, J. Crystal Growth 204 (1999) 512.

[7] S.A. de Vries, P. Goedtkindt, S.L. Bennett, W.J. Huisman, M.J. Zwanenburg, D.-M. Smilgies, J.J. De Yoreo, W.J.P. van Enckevort, P. Bennema, E. Vlieg, Phys. Rev. Lett. 80 (1998) 2229.

[8] P.E. Miller, Lawrence Livermore National Labs Internal Memo NIF0101124 (2003).

[9] K. Sangwal, J. Torrent- Burgues, P. Gorostiza, F. Sanz, Cryst. Res. Technol. 34 (1999) 667.

[10] E. A. Salter, A. Wierzbicki, T. Land, Int. J. Quant. Chem., in press.

[11] Cerius4.2, Accelrys Inc., San Diego, California, 2001.

[12] C.C.J. Roothaan, Rev. Mod. Phys. 23 (1951) 69.

[13] Jaguar version 3.5, Schrodinger, Inc., Portland, Oregon, 1998.

[14] P.J. Hay and W.R. Wadt, J. Chem. Phys. 82 (1985) 299.

W.J.P. van Enckevort, A.C.J.F. van den Berg, J. Crystal Growth 183 (1998) 441.

D.L. Ma, D.K. Tafti, R.D. Braatz, Ind. Eng. Chem.Res. 41 (2002) 6217.

B. Dam, P. Bennema, W.J.P. van Enckevort, J. Crystal Growth 74 (1986) 118.

B. Dam, W.J.P. van Enckevort, J. Crystal Growth 69 (1984) 306.

K. Sangwal, Prog. Crystal Growth and Character 32 (1996) 3.

G.M. Loiacono, J.J. Zola, G. Kostecky, J. Crystal Growth 58 (1982) 495.

C. Belouet, E. Dunia, J.F. Petroff, J. Crystal Growth 23 (1974) 243.

N. Kubota
Cryst. Res. Technol. 36 (2001) 749.
Effect of impurities on the growth kinetics of crystals

X. Sun, Y. Fu, Z. Gau, S. Wang, H. Zeng, Y. Ll
Chinese Science Bulletin 46 (2001) 1142.
Effects of impurities on growth habit of KDP crystal

N. Zaitseva, L. Carman, I. Smolsky, R. Torres, M. Yan,
J. Crystal Growth 204 (1999) 512.
The effect of impurities and supersaturation on the rapid growth of KDP crystals

N. Zaitseva, L. Carman, I. Smolsky,
J. Crystal Growth 241 (2002) 363.
Habit control during rapid growth of kdp and dkdp crystals

H.F. Robey, S. Yu Potapenko, K.D. Summerhays
J. Crystal Growth 213 (2000) 340.
"Bending" of steps on rapidly grown KH2PO4 crystals do to …

W.J.P. van Enckevort, A.C.J.F. van den Berg
J. Crystal Growth 183 (1998) 441.
Impurity blocking of crystal growth: a Monte Carlo study

D.L. Ma, D.K. Tafti, R.D. Braatz
Ind. Eng. Chem.Res. 41 (2002) 6217.
High-Resolution Simulation of Multidimensional Crystal Growth

L.N. Rashkovich, N.V. Kronsky
J. Crystal Growth 182 (1997) 434.
Influence of Fe3+ and Al3+ ions on the kinetics of steps on the {100} faces of KDP

T.A. Eremina, N.N. Eremin, V.A. Kuznetsov, N.G. Furmanova, V.S. Urusov
Crystallography Reports 47 (2002) 753.
Simulation of Defects Formed by Cations of Bivalent and Trivalent Metals in the Structure of Potassium Dihydrogen Phosphate: A Computational Technique

T.A. Eremina, N.N. Eremin, V.A. Kuznetsov, T.M. Okhrimenko, N.G. Furmanova, E.P. Efremova, V.S. Urusov
Crystallography Reports 47 (2002) S76.
Characterization of Defects Generated by Di- and Trivalent Cations in the Potassium Dihydrophosphate Structure …

T.A. Eremina, V.A. Kuznetsov, N.N. Eremin, T.M. Okhrimenko, N.G. Furmanova, E.P. Efremova, V.S. Urusov
Crystallography Reports 46 (2001) 989.
Comparative Characterization of Defects Formed by Di- and Trivalent Dopants …

S. Seif, J.-M. Chang, K. Bhat, B. Penn, R.B. Lal
Crystal Growth & Design 1 (2001) 359.
Investigation of Temperature Dependence and Impurity Content on the Growth Rate of KDP Crystals

H.V. Alexandru, C. Berbecaru, Al. Grancea, V. Iov
J. Crystal Growth 166 (1996) 162.
KDP prismatic faces: kinetics and the mechanism of their growth from solutions

Y. Shangfeng, S. Genbo, T. Jing, M. Bengwei, W. Jianmin, L. Zhengdong
J. Crystal Growth 203 (1999) 425.
Surface topography of rapidly grown KH2PO4 crystals with additives …

Y. Shangfeng, S. Genbo, L. Zhengdong, J. Rihong
J. Crystal Growth 197 (1999) 383.
Rapid growth of KH2PO4 crystals in aqueous solution with additives

J. Crystal Growth 225 (2001) 435.
N.Y. Garces, K.T. Stevens, L.E. Halliburton, M. Yan, N.P. Zaitseva, J.J. De Yoreo
Optical absorption and electron paramagnetic resonance of Fe ions in KDP crystals

Figure 1.

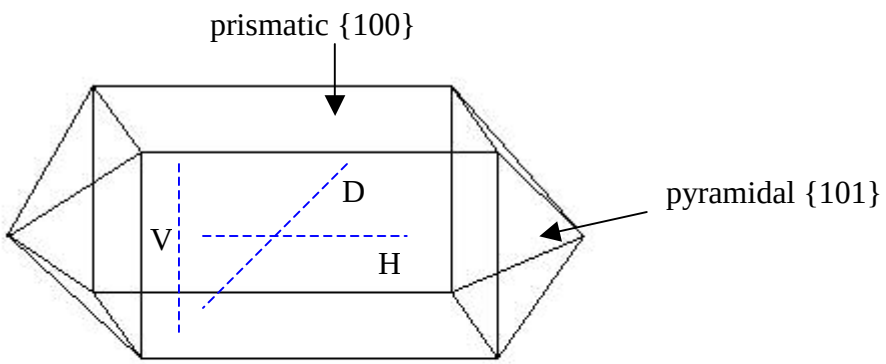

Figure 2.

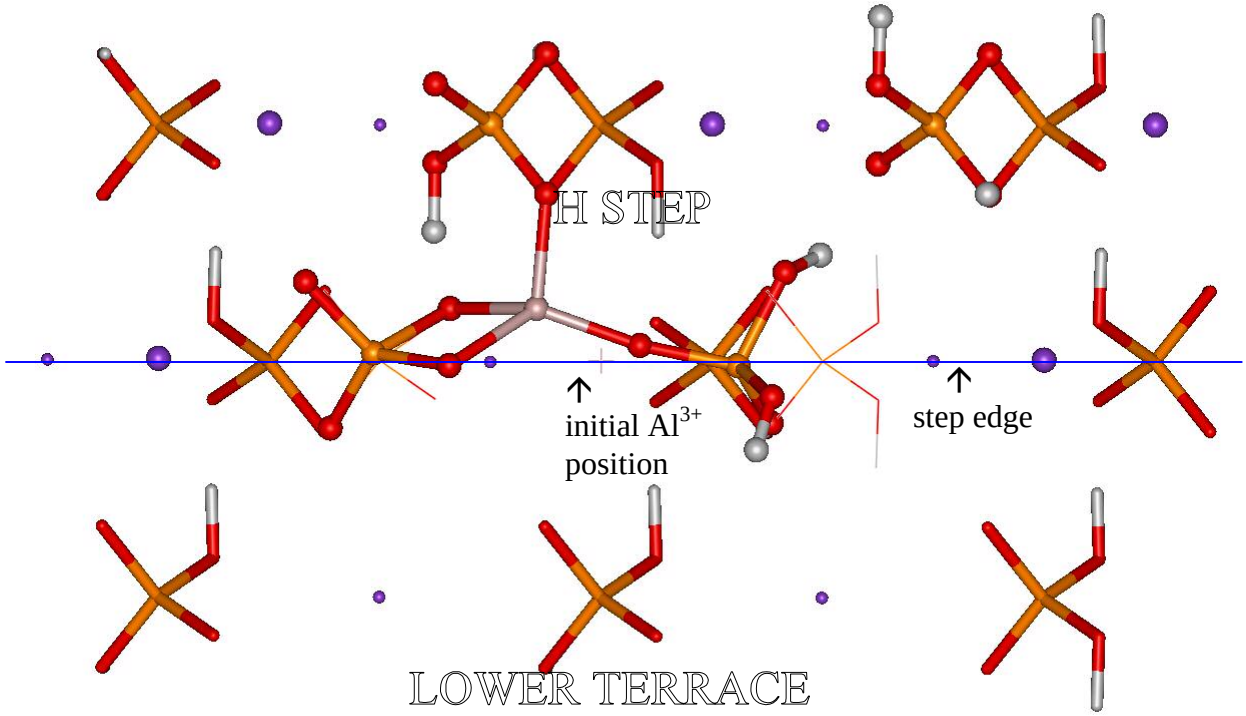

Figure 3a.

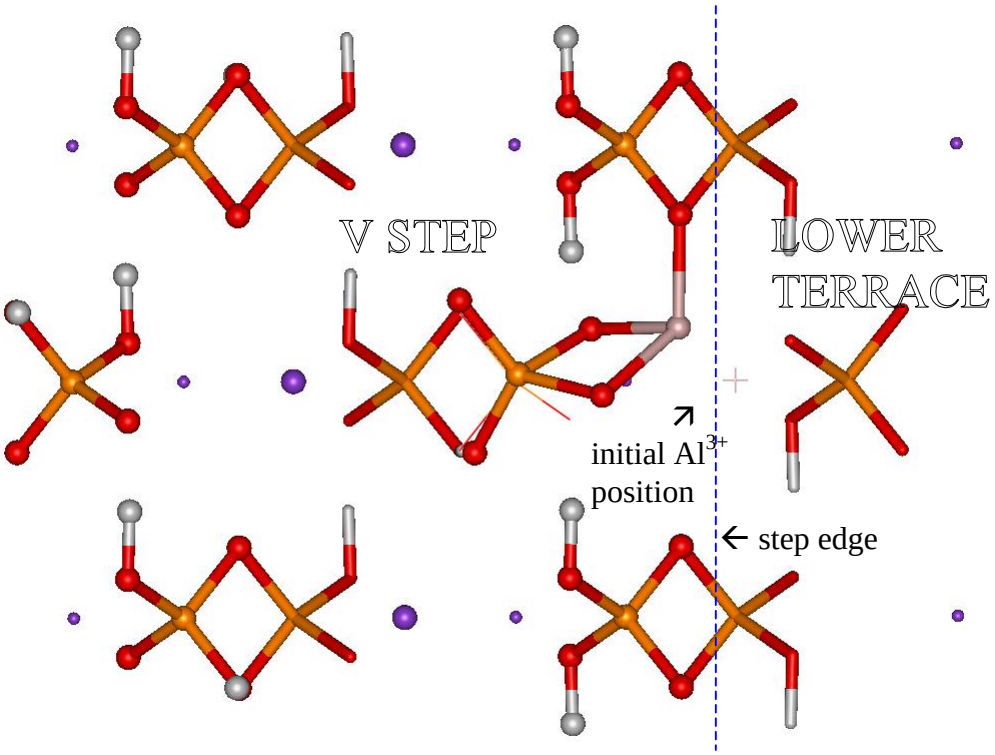

Figure 3b.

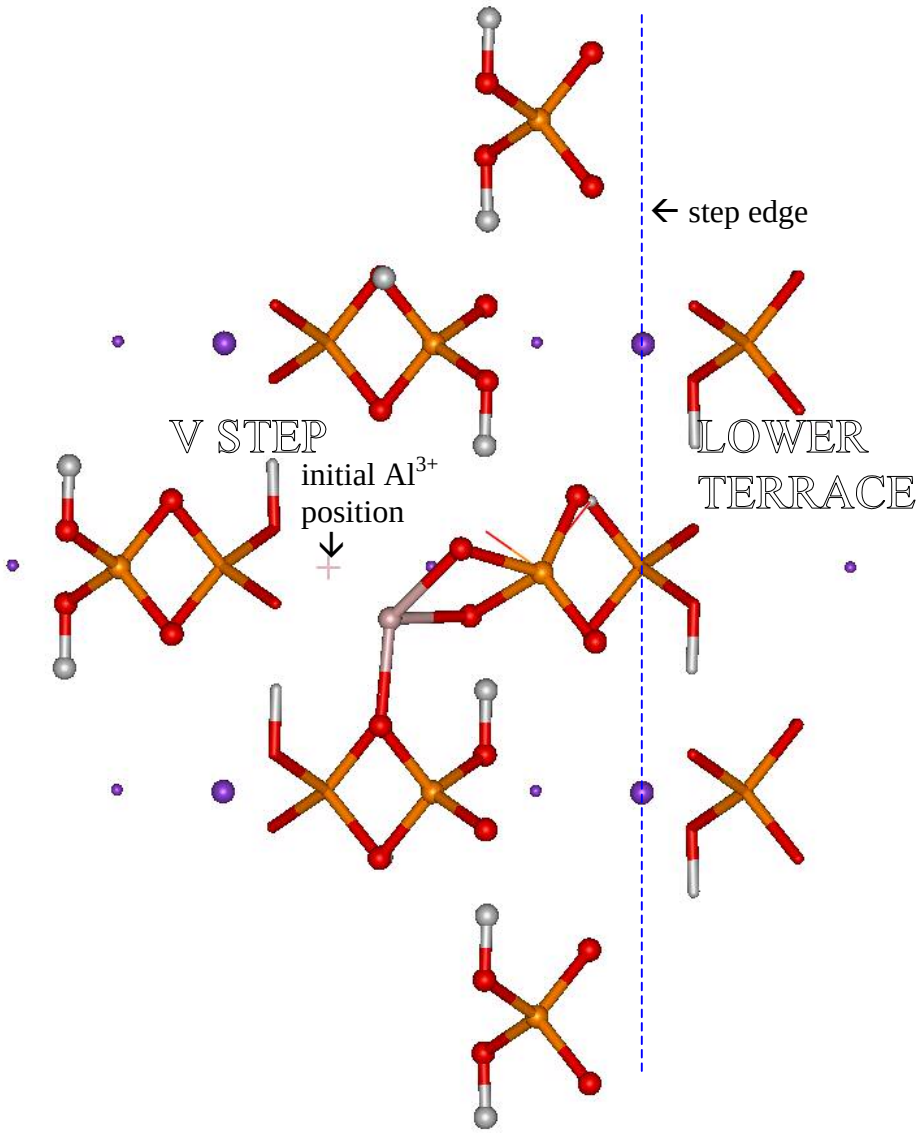

Figure 4.

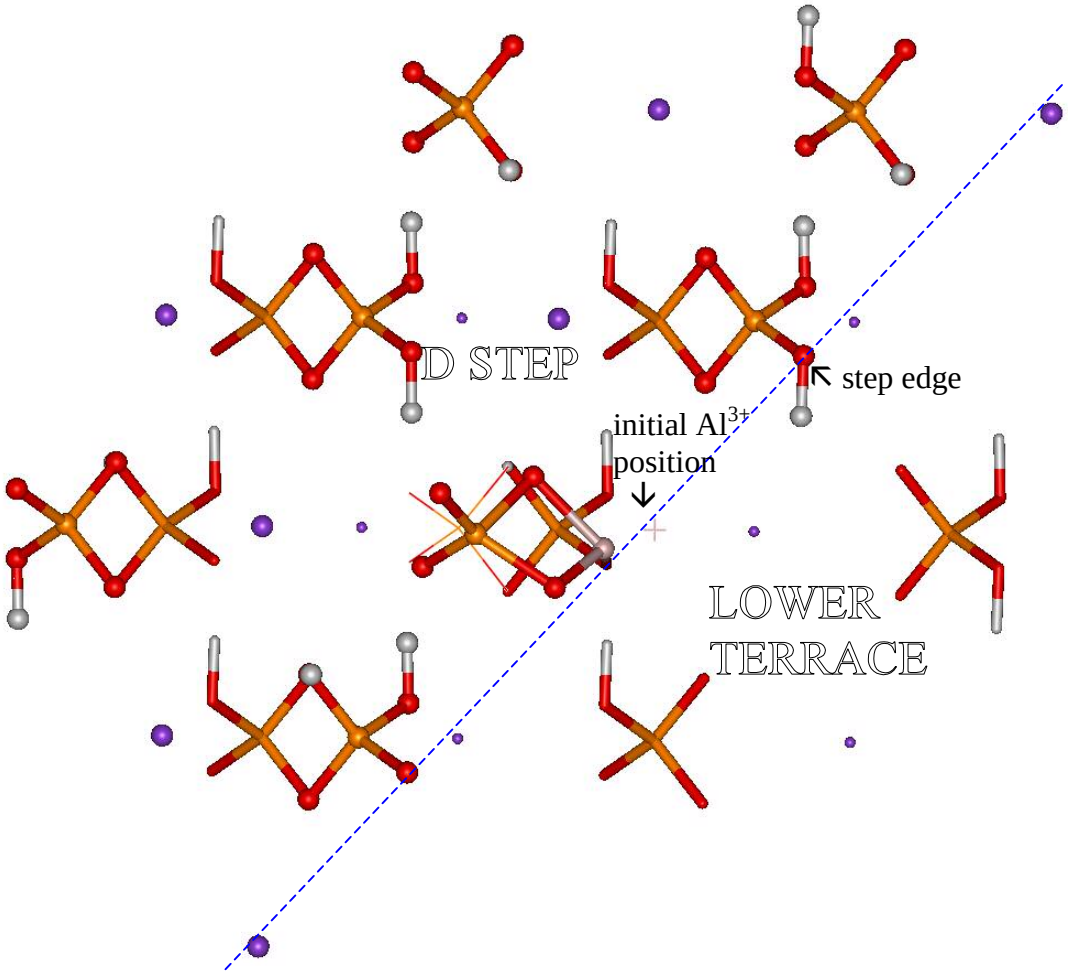

University of California
Lawrence Livermore National Laboratory
Technical Information Department
Livermore, CA 94551